

Efficient optimization method for the light extraction from periodically modulated LEDs using reciprocity

O. T. A. Janssen,* A. J. H. Wachtters, and H. P. Urbach

*Optics Group, Delft University of Technology
Delft, The Netherlands*

o.t.a.janssen@tudelft.nl

Abstract: The incoherent emission of periodically structured Light Emitting Diodes (LEDs) can be computed at relatively low computational cost by applying the reciprocity method. We show that by another application of the reciprocity principle, the structure of the LED can be optimized to obtain a high emission. We demonstrate the method by optimizing one-dimensional grating structures. The optimized structures have twice the extraction efficiency of an optimized flat structure.

© 2010 Optical Society of America

OCIS codes: (050.1755) Computational electromagnetic methods; (050.1950) Diffraction gratings; (050.5298) Photonic crystals; (230.3670) Light-emitting diodes.

References and links

1. T. Fujii, Y. Gao, R. Sharma, E. L. Hu, S. P. DenBaars, and S. Nakamura, "Increase in the extraction efficiency of GaN-based light-emitting diodes via surface roughening," *Appl. Phys. Lett.* **84**(6), 855–857 (2004).
2. M. Boroditsky, T. F. Krauss, R. Coccioli, R. Vrijen, R. Bhat, and E. Yablonovitch, "Light extraction from optically pumped light-emitting diode by thin-slab photonic crystals," *Appl. Phys. Lett.* **75**(8), 1036–1038 (1999).
3. W. J. Choi, Q. H. Park, D. Kim, H. Jeon, C. Sone, and Y. Park, "FDTD Simulation for Light Extraction in a GaN-Based LED," *J. Korean Phys. Soc.* **49**, 877–880 (2006).
4. Y. J. Lee, S. H. Kim, G. H. Kim, Y. H. Lee, S. H. Cho, Y. W. Song, Y. C. Kim, and Y. R. Do, "Far-field radiation of photonic crystal organic light-emitting diode," *Opt. Express* **13**(15), 5864–5870 (2005).
5. H. Rigneault, F. Lemarchand, and A. Sentenac "Dipole radiation into grating structures," *J. Opt. Soc. Am. A* **17**(6), 1048–1058 (2000).
6. A. L. Fehrembach, S. Enoch, and A. Sentenac, "Highly directive light sources using two-dimensional photonic crystal slabs," *Appl. Phys. Lett.* **79**(26), 4280–4282 (2001).
7. A. David, H. Benisty, and C. Weisbuch, "Optimization of Light-Diffracting Photonic-Crystals for High Extraction Efficiency LEDs," *J. Disp. Technol.* **3**(2), 133–148 (2007).
8. A. Roger, and D. Maystre, "Inverse scattering method in electromagnetic optics- Application to diffraction gratings," *J. Opt. Soc. Am.* **70**(12), 1483-1495 (1980).
9. S. J. Norton, "Iterative inverse scattering algorithms: Methods of computing Frechet derivatives," *J. Acoust. Soc. Am.* **106**(5), 2653–2660 (1999).
10. L. D. Landau, and E. M. Lifshitz, *Electrodynamics of Continuous Media* (Pergamom Press, 1960).
11. R. J. Potton, "Reciprocity in Optics," *Rep. Prog. Phys.* **67**(5), 717–754 (2004).
12. J.-J. Greffet, R. Carminati, "Image formation in near-field optics," *Prog. Surf. Sci.* **56**(3), 133–237 (1997).
13. C. E. Reed, J. Giergiel, J. C. Hemminger, and S. Ushioda, "Dipole radiation in a multilayer geometry," *Phys. Rev. B* **36**(9), 4990–5000 (1987).
14. A. Roger, "Reciprocity theorem applied to the computation of functional derivatives of the scattering matrix," *Electromagnetics* **2**(1), 69–83 (1982).
15. S. Bonnard, P. Vincent, and M. Saillard, "Cross-borehole inverse scattering using a boundary finite-element method," *Inverse Probl.* **14**(3), 521–534 (1998).
16. A. Litman, and K. Belkebir, "Two-dimensional inverse profiling problem using phaseless data," *J. Opt. Soc. Am.* **23**(11), 2737–2746 (2006).

17. E. F. Schubert, *Light-Emitting Diodes* (Cambridge University Press, 2006).
 18. M. Yamanishi, and I. Suemune, "Comment on polarization dependent momentum matrix elements in quantum well lasers," *Jpn. J. Appl. Phys.* **23**(Part 2, No. 1), L35–L36 (1984).
 19. M. Cui, H. P. Urbach, and D. K. G. de Boer, "Optimization of light extraction from OLEDs," *Opt. Express* **15**(8), 4398–4409 (2007).
 20. D. G. Luenberger, *Optimization by Vector Space Methods* (Wiley-Interscience, 1967).
 21. X. Wei, A. J. Wachtors, and H. P. Urbach, "Finite-element model for three-dimensional optical scattering problems," *J. Opt. Soc. Am.* **24**(3), 866–881 (2007).
 22. J. J. Wierer, A. David, and M. M. Megens, "III-nitride photonic-crystal light-emitting diodes with high extraction efficiency," *Nat. Photonics* **3**(3), 163–169 (2009).
 23. P. B. Johnson, R. W. Christy, "Optical constants of the noble metals," *Phys. Rev. B* **6**(12), 4370–4379 (1972).
 24. S. G. Johnson, S. Fan, P. R. Villeneuve, J. D. Joannopoulos, L. A. Kolodziejski, "Guided modes in photonic crystal slabs," *Phys. Rev. B* **60**(8), 5751–5758 (1999).
-

1. Introduction

There has always been much interest in coupling light in or out of optical gratings. In the last decade, light-emitting diodes (LEDs) and solar cells have attracted much attention. Whereas for LEDs it is desirable that light is efficiently extracted out of the device, in photovoltaics light from the exterior should be absorbed inside the device. For both applications, highly efficient designs are required to fulfill their promise as a sustainable light and energy source for the near future.

The extraction efficiency of new LEDs is often enhanced by patterning the semiconductor-air interface. Good results have been obtained by random surface roughening [1], but there is also much interest in periodic structures i.e. two-dimensional gratings (photonic crystals) [2–4, 6, 7]. In unpatterned LEDs, the light is mostly trapped by total internal reflection and it radiates primarily from the sides of the device. In photonic crystal LEDs, the mode structure of the photonic crystal helps to prevent that light is radiated laterally. However, it does not guarantee that the light radiates into the direction that is desired. This paper focuses on describing an efficient method for optimizing the radiated intensity of LEDs into a desired cone.

The complexity of current designs requires accurate, rigorous, large-scale, three-dimensional (3D) electromagnetic simulations which need a lot of memory and extensive computations. In this paper, we first describe a very efficient method, based on the reciprocity principle, to calculate the radiation in a single direction from a complete photonic crystal LED for any number of incoherent dipoles at any position in the LED. It requires solving only *two* small quasi-periodic scattering problems on a single cell of the periodic structure. The calculation of the entire radiation pattern of an LED is thus split up into many small computational problems, one for each direction of emission and polarization. Each of the simulations can be done on a standard PC, but in practice we use a supercomputer or cluster to run many angles in parallel. Next to computing the far field radiation, we apply the reciprocity to derive a useful expression of the derivative of the radiated intensity with respect to the grating surface. With this expression the radiated intensity in a certain cone is maximized. Our approach is related to the inverse problem of reconstructing shapes of scattering objects in scatterometry. In this field, an initially unknown permittivity distribution or object shape is reconstructed using only limited field or intensity information, such as far field scattering information. Several of such methods have been developed for gratings [8] and for more general object shapes [9]. Our formulation is specifically derived for structures which contain incoherent sources such as LEDs.

In classical electrodynamics, the electric field \mathbf{E} radiated by a time-harmonic current density \mathbf{J} is derived. The relationship between the field and the source remains unchanged if one interchanges the position of the source and that of the observer. This so-called Lorentz reciprocity

principle can be written as

$$\iiint \mathbf{E}_{\mathbf{J}_1} \cdot \mathbf{J}_2 \, d^3\mathbf{r} = \iiint \mathbf{E}_{\mathbf{J}_2} \cdot \mathbf{J}_1 \, d^3\mathbf{r}, \quad (1)$$

where all quantities are complex field amplitudes. A concise derivation of the reciprocity principle can be found in [10], while in [11] an overview is given of the application of the reciprocity theorem in optics. The theorem is valid for absorbing and anisotropic media, but in general not for nonlinear and active media. In [13], it is suggested that the reciprocity principle can be used to calculate the radiation of a single dipole in a planar dielectric stack. In the field of near-field imaging [12], reciprocity is specifically used for extended incoherent sources. For photonic crystal LEDs, the theorem is applied in combination with a rigorous modal simulation method in [5] and also in [6] to design a highly directive light source. The efficient calculation of the derivative of the radiated intensity using the reciprocity principle is based on the adjoint method, described in [14]. It is used for inverse scattering problems in for instance [15, 16].

In this paper, we first describe in Section 2 the efficient use of the reciprocity principle for computing the emission pattern of incoherent sources in periodic structures and apply this to LEDs. Although interesting in itself, we moreover need this derivation in the iterative optimization of the topography of the LED, which is the topic of Section 3. In Section 4 we discuss LED topographies consisting of one-dimensional gratings that have been optimized by our method.

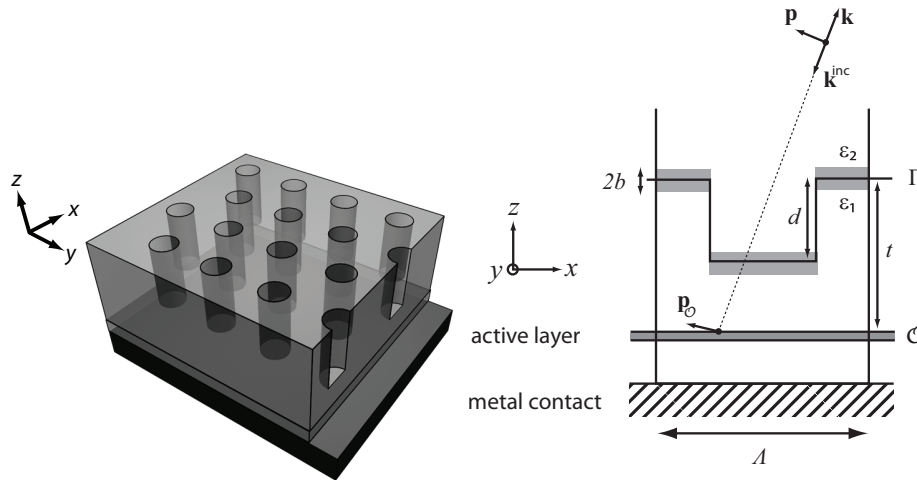


Fig. 1. (left) A typical photonic crystal LED geometry. (right) Schematic of one periodic cell with pitch Λ of a periodic LED. Two different dipole sources \mathbf{p}_O and \mathbf{p} are shown, one in the active layer O and the other in the half-space above interface Γ .

2. The emission from an LED

The LEDs described in this paper consist of a metal contact layer that is covered by one or more layers of semiconductor material (Fig. 1) defined in 3D space with unit vectors $\hat{\mathbf{x}}$, $\hat{\mathbf{y}}$, and $\hat{\mathbf{z}}$ as defined in the figure. Here and in the following, $\hat{\mathbf{a}}$ on a bold face character denotes a vector of unit length. To improve the emission efficiency, the interface Γ between the top-most semiconductor and the surrounding medium is in general not flat. We will specifically discuss the class of interfaces that are periodic in both horizontal directions x and y , though

this periodicity is not a requirement for the computational method that we use and describe. Within the semiconductor region, there is a thin region \mathcal{O} that is the active layer. In this layer, incoherent dipole sources are generated from multiple quantum well structures [17].

To calculate the far-field emission of an LED, we first consider the radiation in the direction of the unit vector $\hat{\mathbf{k}}$ of a single dipole with dipole moment $\mathbf{p}_\mathcal{O}$, oscillating at frequency ω , and situated at point $\mathbf{r}_{\mathbf{p}_\mathcal{O}}$ in the active layer. The corresponding current source density is: $\mathbf{J}_{\mathbf{p}_\mathcal{O}} = -i\omega\mathbf{p}_\mathcal{O}\delta(\mathbf{r} - \mathbf{r}_{\mathbf{p}_\mathcal{O}})$ and radiates the field denoted by $\mathbf{E}_{\mathbf{p}_\mathcal{O}}(\mathbf{r})$. Let $\mathbf{r}_\mathbf{p} = \hat{\mathbf{k}}r_\mathbf{p}$ be a point in the half-space above the LED and let there be a time harmonic dipole at $\mathbf{r}_\mathbf{p}$ with frequency ω and dipole moment \mathbf{p} . The electric field radiated by the latter dipole will be denoted by $\mathbf{E}_\mathbf{k}$. The two sources and radiated fields satisfy the reciprocity principle:

$$\mathbf{E}_{\mathbf{p}_\mathcal{O}}(\hat{\mathbf{k}}r_\mathbf{p}) \cdot \mathbf{p} = \mathbf{E}_\mathbf{k}(\mathbf{r}_{\mathbf{p}_\mathcal{O}}) \cdot \mathbf{p}_\mathcal{O}. \quad (2)$$

If $r_\mathbf{p}$ is sufficiently large, the field that is emitted by \mathbf{p} and that is incident on the LED can be approximated by the field of a spherical wave with electric field vector:

$$\mathbf{E}_\mathbf{k}^{\text{inc}}(\mathbf{r}) = \frac{k^2}{4\pi\epsilon_0 r} e^{ikr} e^{-ik(\hat{\mathbf{k}}\cdot\mathbf{r})} (\hat{\mathbf{k}} \times \mathbf{p}) \times \hat{\mathbf{k}}, \quad (3)$$

which for large distances r from the source is incident as a plane wave. The wave vector of this incident plane wave is $\mathbf{k}^{\text{inc}} = -k\hat{\mathbf{k}} = -k_0\sqrt{\epsilon_2}\hat{\mathbf{k}} = -\mathbf{k}$, where $k_0 = \omega/c$ is the wave number in vacuum and ϵ_2 is the relative permittivity in the half-space above the LED. The vector \mathbf{k}^{inc} points, of course, in the direction opposite to the direction of emission $\hat{\mathbf{k}}$ in which the field radiated by dipole $\mathbf{p}_\mathcal{O}$ is observed. Without restricting the generality we may assume that \mathbf{p} is perpendicular to \mathbf{k}^{inc} . Then the incident field given by Eq. (3) can be simplified to

$$\mathbf{E}_\mathbf{k}^{\text{inc}}(\mathbf{r}) = \frac{k^2}{4\pi\epsilon_0 r} e^{ikr} e^{i\mathbf{k}^{\text{inc}}\cdot\mathbf{r}} \mathbf{p}. \quad (4)$$

The plane of incidence of this plane wave is through \mathbf{k}^{inc} and $\hat{\mathbf{z}}$ (see Fig. 1). It suffices to consider two linear independent polarization states of the incident plane wave. We choose for \mathbf{p} the unit vectors $\hat{\mathbf{v}} = \hat{\mathbf{S}}, \hat{\mathbf{P}}$ corresponding to the S- and P-polarization respectively.

The fields at the location of dipole $\mathbf{p}_\mathcal{O}$ in the active layer due to an incident S- and P-polarized plane wave is found by solving the two separate simulations the two boundary value problems defined by:

$$\omega^2\mu_0\epsilon(\mathbf{r})\mathbf{E}_\mathbf{k}^v(\mathbf{r}) - \nabla \times \nabla \times \mathbf{E}_\mathbf{k}^v(\mathbf{r}) = 0, \quad \mathbf{E}_\mathbf{k}^v(\mathbf{r}) - \mathbf{E}_\mathbf{k}^{\text{inc},v}(\mathbf{r}) \text{ satisfies the o.r.c.}, \quad (5)$$

with $v = S, P$. Here o.r.c. stands for the ‘‘outgoing radiation conditions’’ that apply to the scattered fields, i.e. to the total fields minus the incident fields. For a periodically varying surface Γ as shown in Fig. 1, the fields $\mathbf{E}_\mathbf{k}^v(\mathbf{r})$ are quasi-periodic, so that only a single periodic cell has to be considered with appropriate quasi-periodic boundary conditions. Note that this method does *not* require periodicity of the domain, but for periodic domains only one cell has to be considered.

When the solutions $\mathbf{E}_\mathbf{k}^S(\mathbf{r})$ and $\mathbf{E}_\mathbf{k}^P(\mathbf{r})$ have been computed numerically, the $\hat{\mathbf{S}}$ and $\hat{\mathbf{P}}$ component of the field radiated by dipole $\mathbf{p}_\mathcal{O}$ at $\mathbf{r}_{\mathbf{p}_\mathcal{O}}$ in the direction $\hat{\mathbf{k}}$ follows from reciprocity principle in Eq. (1):

$$\lim_{r_\mathbf{p} \rightarrow \infty} \mathbf{E}_{\mathbf{p}_\mathcal{O}}(r_\mathbf{p}\hat{\mathbf{k}}) \cdot \hat{\mathbf{v}} = \mathbf{E}_\mathbf{k}^v(\mathbf{r}_{\mathbf{p}_\mathcal{O}}) \cdot \mathbf{p}_\mathcal{O}. \quad (6)$$

Using that $\hat{\mathbf{S}}$ and $\hat{\mathbf{P}}$ are orthonormal, the total radiated intensity at $r \rightarrow \infty$ in the direction of $\hat{\mathbf{k}}$ due to dipole $\mathbf{p}_\mathcal{O}$ is proportional to:

$$\lim_{r_\mathbf{p} \rightarrow \infty} |\mathbf{E}_{\mathbf{p}_\mathcal{O}}(r_\mathbf{p}\hat{\mathbf{k}})|^2 = \lim_{r_\mathbf{p} \rightarrow \infty} \sum_{v=S,P} |\mathbf{E}_{\mathbf{p}_\mathcal{O}}(r_\mathbf{p}\hat{\mathbf{k}}) \cdot \hat{\mathbf{v}}|^2 = \sum_{v=S,P} |\mathbf{E}_\mathbf{k}^v(\mathbf{r}_{\mathbf{p}_\mathcal{O}}) \cdot \mathbf{p}_\mathcal{O}|^2. \quad (7)$$

The time-averaged intensity in the direction of $\hat{\mathbf{k}}$ due to incoherent dipoles at $\mathbf{r}_{\mathbf{p}_\ell}$ with random orientation of the dipole vector \mathbf{p}_ℓ , is obtained by integrating Eq. (7) over all directions of \mathbf{p}_ℓ . By substituting $\mathbf{p}_\ell = p_\ell (\cos \phi \sin \theta \hat{\mathbf{x}} + \sin \phi \sin \theta \hat{\mathbf{y}} + \cos \theta \hat{\mathbf{z}})$ into Eq. (7) and averaging over the unit sphere of directions for \mathbf{p}_ℓ , we obtain for the intensity emitted in the direction $\hat{\mathbf{k}}$ per solid angle due to randomly isotropically oriented dipoles at $\mathbf{r}_{\mathbf{p}_\ell}$ with all the same strength p_ℓ :

$$\begin{aligned} I(\mathbf{k}, \mathbf{r}_{\mathbf{p}_\ell}) &= \frac{1}{2} \sqrt{\frac{\epsilon_0 \epsilon_2}{\mu_0}} \frac{1}{4\pi} \int_0^{2\pi} \int_0^\pi \sum_{v=S,P} |\mathbf{E}_{\mathbf{k}}^v(\mathbf{r}_{\mathbf{p}_\ell}) \cdot \mathbf{p}_\ell|^2 \sin \theta \, d\theta \, d\phi \\ &= \frac{p_\ell^2}{6} \sqrt{\frac{\epsilon_0 \epsilon_2}{\mu_0}} \sum_{v=S,P} |\mathbf{E}_{\mathbf{k}}^v(\mathbf{r}_{\mathbf{p}_\ell})|^2. \end{aligned} \quad (8)$$

This result is valid for isotropically oriented dipoles only. For LEDs using multiple quantum well structures it is known, however, that the dipoles are mainly oriented in the plane of the active layer [18]. In that case $\theta = \pi/2$ and averaging should be done over $0 \leq \phi \leq 2\pi$, yielding:

$$\begin{aligned} \tilde{I}(\mathbf{k}, \mathbf{r}_{\mathbf{p}_\ell}) &= \frac{1}{2} \sqrt{\frac{\epsilon_0 \epsilon_2}{\mu_0}} \frac{1}{2\pi} \int_0^{2\pi} \sum_{v=S,P} |\mathbf{E}_{\mathbf{k}}^v(\mathbf{r}_{\mathbf{p}_\ell}) \cdot \mathbf{p}_\ell|^2 \, d\phi \\ &= \frac{p_\ell^2}{4} \sqrt{\frac{\epsilon_0 \epsilon_2}{\mu_0}} \sum_{v=S,P} (|E_{\mathbf{k},x}^v(\mathbf{r}_{\mathbf{p}_\ell})|^2 + |E_{\mathbf{k},y}^v(\mathbf{r}_{\mathbf{p}_\ell})|^2). \end{aligned} \quad (9)$$

To be specific and for simplicity, we shall use Eq. (8) for the radiation pattern. In the radiation cones considered in this paper, dipoles oriented along the z -axis have a minimal influence on the radiation efficiency. Hence, we assume that the dipoles are isotropically oriented. In case this is not true, only minor modification of the derivations need to be carried out. The total intensity radiated in the direction of $\hat{\mathbf{k}}$ per solid angle of randomly oriented incoherent dipoles with fixed length $p_\ell^2 = 6\sqrt{\mu_0/\epsilon_0\epsilon_2}$ in the entire active layer \mathcal{O} is found by integrating $\mathbf{r}_{\mathbf{p}_\ell}$ over the active layer:

$$I(\hat{\mathbf{k}}) = \iiint_{\mathcal{O}} \sum_{v=S,P} |\mathbf{E}_{\mathbf{k}}^v(\mathbf{r}_{\mathbf{p}_\ell})|^2 \, d^3 \mathbf{r}_{\mathbf{p}_\ell}. \quad (10)$$

Writing $\hat{\mathbf{k}} = \cos \phi_{\hat{\mathbf{k}}} \sin \theta_{\hat{\mathbf{k}}} \hat{\mathbf{x}} + \sin \phi_{\hat{\mathbf{k}}} \sin \theta_{\hat{\mathbf{k}}} \hat{\mathbf{y}} + \cos \theta_{\hat{\mathbf{k}}} \hat{\mathbf{z}}$, the total radiation emitted inside the cone $0 \leq \theta_{\hat{\mathbf{k}}} \leq \theta_C$, with solid angle $\Omega = 2\pi(1 - \cos \theta_C)$, is given by

$$I(\Omega) = \int I(\hat{\mathbf{k}}) \, d\Omega, \quad (11)$$

where $d\Omega = r^2 \sin \theta_{\hat{\mathbf{k}}} d\theta_{\hat{\mathbf{k}}} d\phi_{\hat{\mathbf{k}}}$. To compute the integral numerically, $I(\hat{\mathbf{k}})$ has to be calculated for sufficiently many $\theta_{\hat{\mathbf{k}}}$, $\phi_{\hat{\mathbf{k}}}$. Each angle requires solving two quasi-periodic rigorous scattering problems.

3. Optimization of the LED surface

For the radiation pattern and the total radiated energy of an LED, the shape and position of the surface Γ is essential. The main goal is to find a suitable Γ for the application under consideration. For simplicity, we restrict ourselves in this paper to a two-dimensional LED-like geometry, i.e. the interface Γ is translational invariant with respect to y and hence is specified by a periodic curve $z = \Gamma(x) = \Gamma(x + \Lambda)$, with Λ the period. The radiating sources are in this two-dimensional situation current wires parallel to the y -axis. In addition, all quantities are per unit length in the y -direction. The full three-dimensional case can be tackled in the same manner as the two-dimensional case.

The assumption of radiation current lines implies that all dipoles along these wires are coherent. It can be shown that in a homogeneous medium when the dipole moments are in the y -direction, i.e. the current is parallel to the wire, the radiation pattern of these coherent dipoles is identical to that of incoherent dipoles [19]. For dipoles oriented in other directions than the y -direction, there is a difference between the radiation pattern of the coherent and incoherent case. However, this difference is not large in a two-dimensional configuration.

First, we suppose that the transition of the permittivity function across the interface is smooth. To be more specific, we choose $b > 0$ and define for a configuration with surface Γ the permittivity function $\varepsilon(\Gamma)(x, z)$ by:

$$\varepsilon(\Gamma)(x, z) = \begin{cases} \varepsilon_0 \varepsilon_1 & \text{for } z \leq \Gamma(x) - b; \\ \varepsilon_0 \varepsilon_2 & \text{for } z \geq \Gamma(x) + b; \\ \text{smooth} & \text{for } \Gamma(x) - b \leq z \leq \Gamma(x) + b. \end{cases} \quad (12)$$

The permittivity varies then smoothly in the strip S_b^Γ defined by:

$$S_b^\Gamma = \{(x, z), 0 \leq x \leq a, \Gamma(x) - b \leq z \leq \Gamma(x) + b\}. \quad (13)$$

In the end, we will let $b \rightarrow 0$ to represent a sharp transition, but until stated otherwise $\varepsilon(\Gamma)$ is smooth for fixed $b > 0$. For a given surface Γ , the quantity that we intend to maximize is the energy emitted in a specific direction given by the unit vector $\hat{\mathbf{k}}$. Obviously, we can just as well maximize the energy emitted inside the entire cone, but to keep the notation concise we choose to optimize only a single direction. Hence we maximize

$$I(\Gamma) = \sum_{\nu=S,P} \iint_{\mathcal{O}} |\mathbf{E}^\nu(\Gamma)|^2 dx dz, \quad (14)$$

where $\mathbf{E}^\nu(\Gamma)$ is the electric field due to an incident plane wave with unit amplitude and direction of incidence given by $-\hat{\mathbf{k}}$. The plane wave is either S- or P-polarized. Only one case of polarization is considered, the other can be dealt with in the same way, so that we omit in the following the superscript ν from the electric field vectors due to an incident plane wave and of the incident field itself. The field $\mathbf{E}(\Gamma)$ is computed by solving a single diffraction problem defined by Eq. (5). From the theory of reciprocity, $I(\Gamma)$ is also the contribution of one polarization to the averaged intensity emitted by mutually incoherent wires in the active region, radiated in the single direction specified by $\hat{\mathbf{k}}$ as described in the previous section.

We are interested in increasing this intensity by varying the surface by a perturbation $\xi h(x)$, leading to a new surface $\Gamma(x) \rightarrow \Gamma(x) + \xi h(x)$, with $\xi > 0$. Since $z = h(x)$ is a function we use the Gateaux derivative [20] which in the direction h is given by

$$\delta I(\Gamma; h) = \lim_{\xi \rightarrow 0} \frac{1}{\xi} [I(\Gamma + \xi h) - I(\Gamma)] = 2\text{Re} \left[\iint_{\mathcal{O}} \delta \mathbf{E}(\Gamma; h) \cdot \mathbf{E}(\Gamma)^* dx dz \right], \quad (15)$$

where $\delta \mathbf{E}(\Gamma; h)$ is the Gateaux derivative of the electric field $\mathbf{E}(\Gamma)$ in the direction of h , and $*$ denotes the complex conjugate. To obtain $\delta \mathbf{E}(\Gamma; h)$ we consider two electromagnetic boundary value problems. The first is that of an incident plane wave \mathbf{E}^{inc} on an LED with surface Γ as described by Eq. (5) and the second is that of the same incident plane wave on an LED with surface $\Gamma + \xi h$:

$$\omega^2 \mu_0 \varepsilon(\Gamma) \mathbf{E}(\Gamma) - \nabla \times \nabla \times \mathbf{E}(\Gamma) = 0, \quad \mathbf{E}(\Gamma) - \mathbf{E}^{\text{inc}} \text{ satisfies the o.r.c.} \quad (16)$$

$$\omega^2 \mu_0 \varepsilon(\Gamma + \xi h) \mathbf{E}(\Gamma + \xi h) - \nabla \times \nabla \times \mathbf{E}(\Gamma + \xi h) = 0, \quad \mathbf{E}(\Gamma + \xi h) - \mathbf{E}^{\text{inc}} \text{ satisfies the o.r.c.} \quad (17)$$

with in both cases quasi-periodic boundary conditions on the sides ($x = 0, x = \Lambda$) of the cell. By subtracting Eq. (17) from Eq. (16) we get

$$\begin{aligned} \omega^2 \mu_0 \varepsilon(\Gamma) [\mathbf{E}(\Gamma) - \mathbf{E}(\Gamma + \xi h)] - \nabla \times \nabla \times [\mathbf{E}(\Gamma) - \mathbf{E}(\Gamma + \xi h)] \\ = \omega^2 \mu_0 [\varepsilon(\Gamma + \xi h) - \varepsilon(\Gamma)] \mathbf{E}(\Gamma + \xi h), \end{aligned} \quad (18)$$

$\mathbf{E}(\Gamma) - \mathbf{E}(\Gamma + \xi h)$ satisfies the o.r.c.

Equation (18) is inhomogeneous with a source term that is non-zero exactly there where the permittivity function is altered by the perturbation. We shall take the limit $\xi \rightarrow 0$ of Eq. (18). For the permittivity difference on the right-hand-side of Eq. (18), we note that, since $\varepsilon(\Gamma + \xi h)$ is the function $\varepsilon(\Gamma)$ translated by $-\xi h(x)$ parallel to the z -axis, we have

$$\varepsilon(\Gamma + \xi h)(x, z) = \varepsilon(\Gamma)(x, z - \xi h(x)) \quad \text{for all } x, z. \quad (19)$$

Hence, in the limit $\xi \rightarrow 0$ the permittivity difference becomes, according to the definition of the derivative, proportional to its partial derivative with respect to the z coordinate:

$$\begin{aligned} \lim_{\xi \rightarrow 0} [\varepsilon(\Gamma + \xi h)(x, z) - \varepsilon(\Gamma)(x, z)] &= \lim_{\xi \rightarrow 0} [\varepsilon(\Gamma)(x, z - \xi h(x)) - \varepsilon(\Gamma)(x, z)] \\ &= -\frac{\partial \varepsilon(\Gamma)}{\partial z}(x, z) h(x) \mathbb{1}_{S_b^\Gamma}(x, z), \end{aligned} \quad (20)$$

where $\mathbb{1}_{S_b^\Gamma}(x, z)$ is the function that is 1 in the region S_b^Γ and 0 otherwise. Hence, Eq. (18) becomes in the limit $\xi \rightarrow 0$:

$$\begin{aligned} \omega^2 \mu_0 \varepsilon(\Gamma) \delta \mathbf{E}(\Gamma; h) - \nabla \times \nabla \times \delta \mathbf{E}(\Gamma; h) &= \omega^2 \mu_0 \frac{\partial \varepsilon(\Gamma)}{\partial z} h \mathbf{E}(\Gamma) \mathbb{1}_{S_b^\Gamma}. \end{aligned} \quad (21)$$

$\delta \mathbf{E}(\Gamma; h)$ satisfies the o.r.c.

We conclude that $\delta \mathbf{E}(\Gamma; h)$ is the electric field radiated by the current density defined by

$$\mathbf{J}_\Gamma(x, z) = i\omega \frac{\partial \varepsilon(\Gamma)}{\partial z}(x, z) h(x) \mathbf{E}(\Gamma)(x, z) \mathbb{1}_{S_b^\Gamma}(x, z), \quad (22)$$

in the configuration with surface Γ . Note that \mathbf{J}_Γ depends linearly on the perturbation h of the interface and is nonzero only inside the strip S_b^Γ that surrounds the curve $z = \Gamma(x)$.

Hence, to compute the Gateaux derivatives $\delta \mathbf{E}(\Gamma; h)$ and therefore $\delta I(\Gamma; h)$ in a particular direction h , one has to solve the radiation problem of Eq. (21). In the optimization algorithm, out of all possible h , the direction of steepest ascent should be found, i.e. the direction \tilde{h} such that $\delta I(\Gamma; \tilde{h})$ is maximum compared to $\delta I(\Gamma; h)$ for all other h of the same norm. By applying again the reciprocity principle in a manner explained below, it turns out that this optimal direction can also be found by solving only *one* radiation problem (per polarization).

To explain this, we first define the current density

$$\mathbf{J}_\mathcal{O} = \mathbf{E}(\Gamma)^* \mathbb{1}_\mathcal{O}. \quad (23)$$

This current is only nonzero in the active region \mathcal{O} . Let the field $\mathbf{E}_{\mathbf{J}_\mathcal{O}}(\Gamma)$ be the electric field that is radiated by this current $\mathbf{J}_\mathcal{O}$ in the configuration with curve Γ . Hence $\mathbf{E}_{\mathbf{J}_\mathcal{O}}(\Gamma)$ satisfies:

$$\begin{aligned} \omega^2 \mu_0 \varepsilon(\Gamma) \mathbf{E}_{\mathbf{J}_\mathcal{O}}(\Gamma) - \nabla \times \nabla \times \mathbf{E}_{\mathbf{J}_\mathcal{O}}(\Gamma) &= -i\omega \mu_0 \mathbf{E}(\Gamma)^* \mathbb{1}_\mathcal{O}, \end{aligned} \quad (24)$$

$\mathbf{E}_{\mathbf{J}_\mathcal{O}}(\Gamma)$ satisfies the o.r.c.

We now use Eq. (23) and the reciprocity principle to rewrite Eq. (15) as follows:

$$\begin{aligned}
\delta I(\Gamma; h) &= 2\text{Re} \left[\iint_{\mathcal{O}} \delta \mathbf{E}(\Gamma; h) \cdot \mathbf{J}_{\mathcal{O}} \, dx dz \right] \\
&= 2\text{Re} \left[\iint \mathbf{J}_{\Gamma} \cdot \mathbf{E}_{\mathbf{J}_{\mathcal{O}}}(\Gamma) \, dx dz \right] \\
&= -2\text{Im} \left[\omega \iint_{S_b^{\Gamma}} \frac{\partial \varepsilon(\Gamma)}{\partial z} h \mathbf{E}(\Gamma) \cdot \mathbf{E}_{\mathbf{J}_{\mathcal{O}}}(\Gamma) \, dx dz \right] \tag{25}
\end{aligned}$$

where the reciprocity principle is used in the second step. From Eq. (25), the Gateaux derivative $\delta I(\Gamma; h)$ can be determined for all perturbations $h(x)$ at a small computational cost. In fact, to compute $\delta I(\Gamma; h)$ for an arbitrary h one only needs to know the fields $\mathbf{E}(\Gamma)$ and $\mathbf{E}_{\mathbf{J}_{\mathcal{O}}}$. To determine these fields one scattering problem (to compute $\mathbf{E}(\Gamma)$) and one radiation problem (to compute $\mathbf{E}_{\mathbf{J}_{\mathcal{O}}}$) have to be solved. Note that when both polarizations S and P are taken into account we need to solve two scattering and two radiation problems, one for every polarization. But once these four problems have been solved, the Gateaux derivative $\delta I(\Gamma; h)$ can be computed for *any* perturbation h by simply computing the integral in Eq. (25).

Let h be normed in some way, e.g. $\int_0^{\Lambda} h(x)^2 \, dx = 1$, then the perturbation \tilde{h} of given norm for which $\delta I(\Gamma; h)$ is maximum is given by the \tilde{h} for which the integral at the right of Eq. (25) is maximum. Since h is only a function of x , \tilde{h} is given by

$$\tilde{h}(x) = -C \text{Im} \left[\int_{\Gamma(x)-b}^{\Gamma(x)+b} \frac{\partial \varepsilon(\Gamma)}{\partial z} (x, z) \mathbf{E}(\Gamma)(x, z) \cdot \mathbf{E}_{\mathbf{J}_{\mathcal{O}}}(x, z) \, dz \right], \tag{26}$$

where C is such that $\int_0^{\Lambda} \tilde{h}(x)^2 \, dx = 1$.

The perturbation \tilde{h} corresponding to the direction of steepest ascent for the case of a permittivity function ε that is discontinuous across Γ is obtained by taking the limit $b \rightarrow 0$ in the previous result. Taking this limit requires a careful analysis of the integral in Eq. (26) in which the components of the electric field that are parallel and perpendicular to the curve Γ have to be considered separately. These components are denoted by $\mathbf{E}_{\parallel}(\Gamma)$, $\mathbf{E}_{\mathbf{J}_{\mathcal{O}, \parallel}}$ and $\mathbf{E}_{\perp}(\Gamma)$, $\mathbf{E}_{\mathbf{J}_{\mathcal{O}, \perp}}$, respectively. The result of taking the limit $b \rightarrow 0$ is then:

$$\begin{aligned}
\tilde{h}(x) &= -C \text{Im} \left[(\varepsilon_2 - \varepsilon_1) \mathbf{E}_{\parallel}(\Gamma)(x, \Gamma(x)) \cdot \mathbf{E}_{\mathbf{J}_{\mathcal{O}, \parallel}}(x, \Gamma(x)) \right. \\
&\quad \left. - \varepsilon_2 \left(1 - \frac{\varepsilon_2}{\varepsilon_1}\right) \mathbf{E}_{\perp}(\Gamma)(x, \Gamma(x)+0) \cdot \mathbf{E}_{\mathbf{J}_{\mathcal{O}, \perp}}(x, \Gamma(x)+0) \right]. \tag{27}
\end{aligned}$$

For the details of the derivation we refer to the Appendix.

Mathematical optimization means to iteratively find values for the degrees of freedom that lead to the largest figure of merit, in our case the radiated intensity. These values are found by systematically trying new values that are chosen such that every next step in the algorithm leads to a higher figure of merit. By choosing $\tilde{h}(x)$ such as defined in Eq. (27) the surface given by $\Gamma(x) + \xi \tilde{h}(x)$ will lead to a higher radiated intensity, provided that the step size ξ is not too big and that $\Gamma(x)$ is not already a local maximum.

4. Results

To compute radiation patterns and the Gateaux derivatives when the curve Γ is optimized electromagnetic boundary value problems on a periodic computational domain have to be solved. Because the computational domain is relatively small (a single period), the problems can be tackled by almost any type of rigorous electromagnetic solvers. For this paper, calculations are performed using an implementation of the Finite Element Method [21].

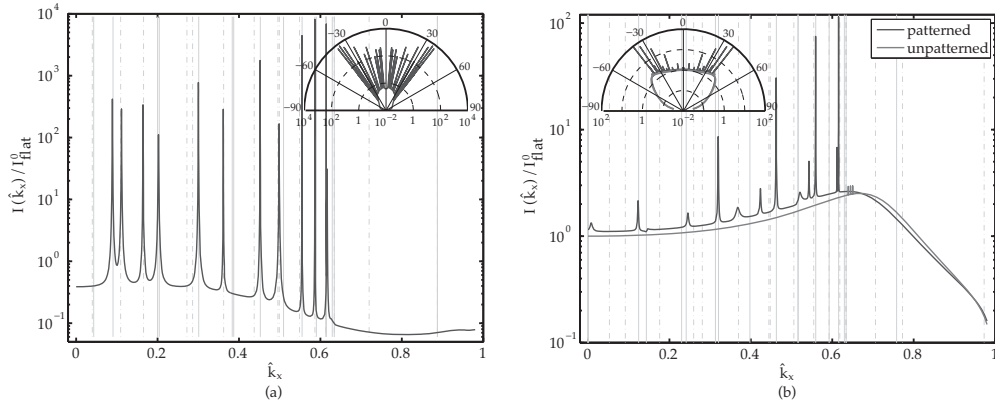


Fig. 2. Angle dependent intensity at the wavelength of 450nm of isotropically radiating dipoles in a geometry with 700nm thick GaN, an active layer 100nm above the metal contact, and a grating with a pitch of 250nm and a depth of 5nm. Values are normalized by the intensity of the flat geometry I_{flat}^0 at $k_x = 0$. The solid and dashed vertical lines depict, respectively, the location of the S and P waveguide modes of the flat geometry. The insets show the corresponding radiation patterns. (a) The metal contact is considered a perfect metallic conductor. (b) The metal contact is considered to be silver (Ag) with complex permittivity.

In Fig. 2 the radiated intensity from a one-dimensional grating with a shallow, 5nm deep, grating is shown. It is calculated using the reciprocity theorem as described in Section 2. The geometry is similar to that described in [22]. It is immediately clear that the resonance peaks resulting from the patterning are sharp and several orders higher than the background intensity of the unpatterned geometry. Assuming that the metallic contact layer is perfectly conducting, the resonances have Q-factors ($Q = k_{\text{max}}/\Delta k_{\text{fwhm}}$) up to 10^5 .

Using tabulated permittivity data of silver [23], the Q-factors reach up to values of the order of 10^3 . These sharp resonances are potentially problematic for the reciprocity calculation method, where for each discrete k_x value a new simulation has to be performed. To capture all the maxima, taking into account a potential Full Width Half Maximum (FWHM) of $\Delta \hat{k}_{\text{fwhm}} = 10^{-6}$, the angles corresponding to $0 \leq \hat{k}_x \leq 1$ would need to be approximated by at least 10^6 reciprocal simulations. Since, the total radiation depends on the correct approximation of these resonances, this computational burden would render the reciprocity method unpractical. However, since simulations can be done per k_x , an adaptive method can be applied. First, a relatively small number of angles (30 to 80 in our case) are simulated. Then a heuristic algorithm determines at what angles additional simulations are required. This is in general close to a local maximum of $I(\hat{k}_x)$ or where the derivative $\partial I(\hat{k}_x)/\partial \hat{k}_x$ is large. New simulations are then performed until all maxima are sufficiently resolved and usually not more than 150 angles are required.

For this shallow grating, the locations of the resonances found correspond well to the guided modes in the GaN layer for the unpatterned geometry with a layer thickness of 698nm (Fig. 2). Although all resonances correspond to a guided mode, not all guided modes result in a radiation maximum. It is well known that for the unpatterned geometry most of the light is guided in the GaN waveguide by total internal reflection and will never couple out into the air region. Reciprocally, this means that with a plane wave we can never excite such a guided mode. For the patterned geometry, most of these modes become leaky and result in radiation. There

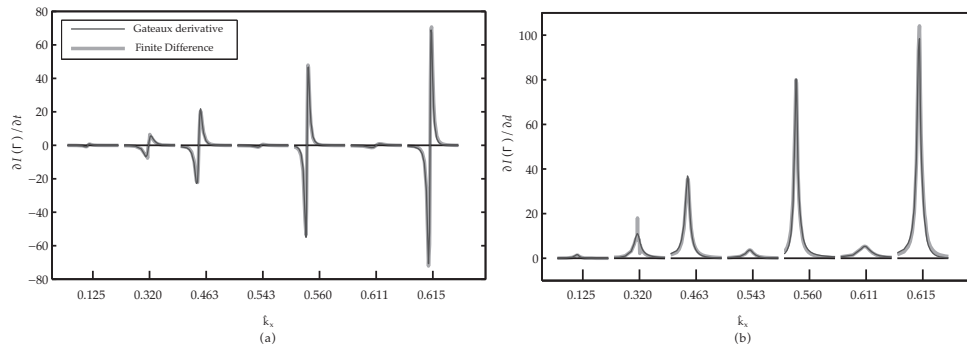


Fig. 3. Gateaux derivative at the surface Γ as defined for Fig. 2. The x -axis is cut as to emphasize the derivative close to the resonances. (a) Gateaux derivative with respect to the average layer thickness t . (b) Gateaux derivative with respect to the grating depth d .

are, however, still guided modes for this geometry that will not contribute to the LED radiation. These resonant modes can be found by a different calculation of the modes in a photonic crystal waveguide [24].

Figure 2 shows that even a very shallow patterning can significantly increase the radiated power over that of the unpatterned geometry and in this case almost all of the enhancement is in a cone with an opening angle of 90° . For most LED applications, it is desired that the enhancement is restricted to even smaller cones.

In Fig. 3 the Gateaux derivative $\delta I(\Gamma; h)$ with respect to the average layer thickness t and grating depth d as indicated in Fig. 1 is shown. From the sign of the derivative it is clear that the radiated intensity of this particular shallow grating can be improved by increasing its depth d . For the average layer thickness it is also clear that the integral of the derivative over all angles is positive and we should try a larger film thickness. However, at every resonance the derivative has a negative and a positive lobe that almost cancel. This again shows that the discretization of the angles is important to obtain an accurate value for the derivative. Because the left lobe is always negative and the right lobe is always positive, the resonant peaks will shift to larger angles if we increase the average layer thickness.

Since this grating is described by only 2 parameters, namely the average layer thickness and the grating depth, it is feasible to find an optimal solution using a brute force method instead of our method based on reciprocity. In Fig. 4 we show the radiated intensity for a large range of geometries. The Fabry-Pérot maxima for the unpatterned geometry are visible in the bottom of the plot i.e. for zero grating depth, with series of weaker and stronger local maxima for deeper patterns. Using the gradient simulations described in the previous section, the 2-dimensional parameter space is also optimized using a simple steepest ascent optimization method with damped step size. Several optimization paths with random starting conditions are also shown in Fig. 4. Using the optimization method based on reciprocity, with the same computational effort, we can scan the optimization space of a surface defined by any number of parameters.

Figures 5(a) and 5(b) show two geometries at local maxima for the extraction efficiency with a surface defined by only 2 parameters (a block grating) and one that is defined by 10 parameters. It is clear from the image that the ideal location of the active layer is in both cases around $z = 120\text{nm}$. This position is mainly determined by the metal boundary and is very insensitive to the actual grating above it. However, for the block grating it is clear that within the patterning there are hot spots where the radiation from incoherent dipoles is much stronger than

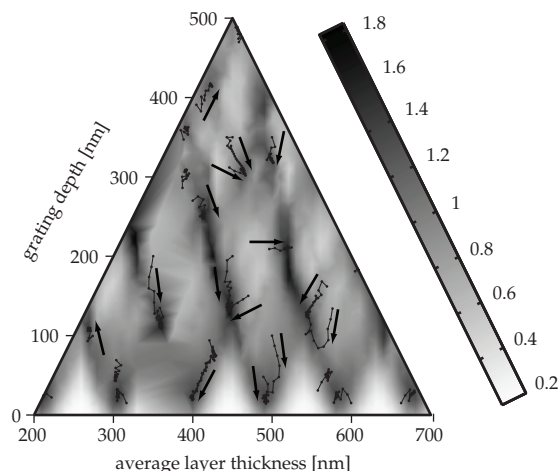


Fig. 4. Radiated intensity of an LED with a block grating and pitch $\Lambda = 450\text{nm}$, normalized to the maximum intensity obtainable with an unpatterned geometry. The indicated paths are optimization paths from arbitrary starting points leading to several local maxima.

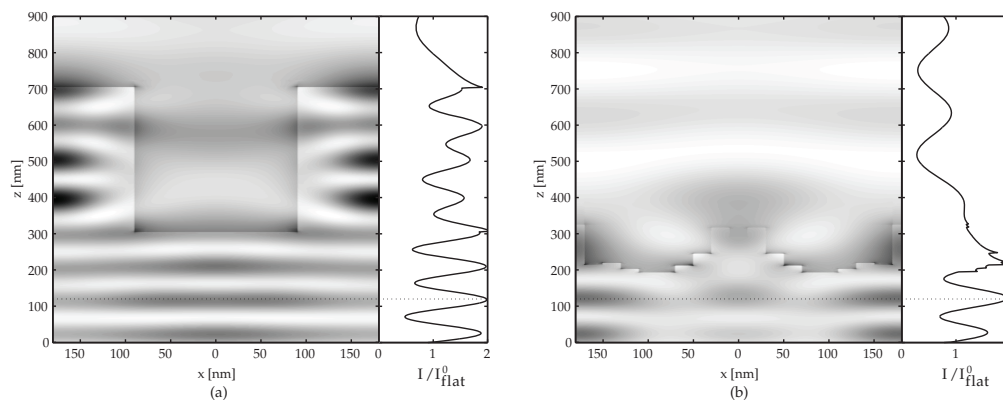


Fig. 5. Plot of the radiated intensity in a cone with 60° opening angle ($k_x < 0.5$) resulting from a local incoherent dipole as a function of its position within the grating. The plot on the right is the radiated intensity of incoherent dipoles in a thin flat active layer at the corresponding z -coordinate. (a) After optimizing with surface 2 parameters. (b) After optimizing a surface parameterized by 10 parameters.

on average in the chosen active layer. The reciprocity method is thus convenient for determining the ideal position of the active layer, provided that we assume that the active layer has a similar refractive index as the surrounding semiconductor.

Similarly, the ideal thickness for the active layer can be found directly from the near-field data. While for semiconductor LEDs the active layer thickness is more or less fixed by the design of the multiple quantum wells, for organic LEDs this extra information can be used to estimate the most effective light-emitting polymer layer thickness. Because the optimization method always ensures that the most radiation occurs from the chosen active layer and its dependence on the z -coordinate is mainly determined by the Fabry-Perot resonance of the incident field in the semiconductor, we chose not to explicitly optimize with respect to the thickness of

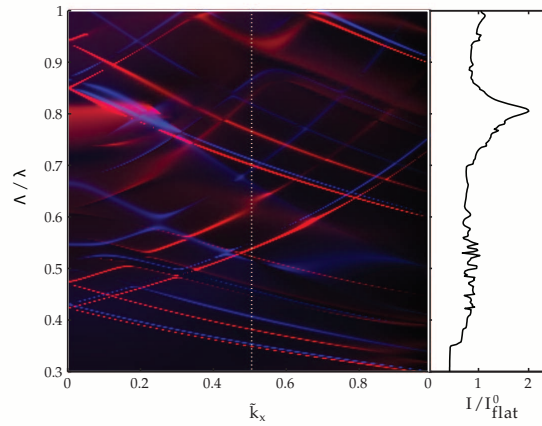


Fig. 6. Radiated intensity of a grating with $t = 700\text{nm}$ and $d = 300\text{nm}$ as a function of the normalized pitch Λ/λ and angle \hat{k}_x . Red shades indicate contributions from p-polarized emission, while blue shades indicate the contribution by s-polarized emission. The plot on the right gives the total radiated intensity in a cone with a 60° opening angle ($\hat{k}_x < 0.5$).

the active layer.

During the optimization, the grating surface is varied causing the radiated energy to be re-distributed over the available resonant modes that can be excited in the structure. In Fig. 6, the angular dependence of the radiated intensity is shown for the optimized structure in Fig. 5(a) as a function of the normalized pitch, being in essence a photonic band diagram. While very sharp resonances exist for all pitches, this does in general not lead to an enhanced extraction compared to the optimal unpatterned geometry. For this geometry, only close to $\Lambda/\lambda = 0.8$ a substantial enhancement occurs. Therefore, next to optimizing the grating surface, an appropriate choice for the pitch is of paramount importance.

An efficient derivative of the radiated intensity with respect to parameters such as the grating period or the angle of incidence is not practical with the method described in this paper. Often an initial guess for the period can be made from fast band structure calculations of photonic crystals. The optimization method is then used to obtain a surface that gives an optimal extraction efficiency for that chosen period. From tests, it is found that optimizing for a slightly perturbed period leads to a similar extraction efficiency for a slightly different surface. The local maxima of radiated intensity are therefore weak in a parameter space that includes both the surface and the period.

5. Conclusions

In conclusion, we have described a very efficient formalism to simulate the light extraction from grating assisted LEDs and to compute an optimal grating surface, both based on the reciprocity principle. To simulate the radiated intensity in a given direction due to the entire active layer only two small-scale boundary value problems have to be solved. Then, only two additional simulation are needed to find the Gateaux derivative with respect to the shape of the LED surface. Using two-dimensional simulations, we have shown that the method can be applied to compute radiation patterns accurately and efficiently. In addition, the data immediately

show at what positions in the LED the active region should be located. The calculated Gateaux derivatives are accurate and are used to optimize the surface of the grating. We believe that by applying this method to full three-dimensional LED geometries, better solutions can be found than are currently available at much less computational costs.

6. Appendix

As stated, Eq. (25) is valid only when $\varepsilon(\Gamma)$ is smooth in the neighborhood of Γ . We now consider the case that the permittivity ε jumps across Γ , by taking the limit $b \rightarrow 0$ in the previous result of Eq. (25). This is rather tricky, because the electric fields $\mathbf{E}(\Gamma)$ and $\mathbf{E}_{\mathbf{J}_\rho}$ are discontinuous across Γ . We therefore first apply a partial integration with respect to z to the integral in Eq. (25) for fixed $b > 0$:

$$\int_0^\Lambda \varepsilon_0 \varepsilon_2 h(x) \mathbf{E}(\Gamma)(x, \Gamma(x)+b) \cdot \mathbf{E}_{\mathbf{J}_\rho}(x, \Gamma(x)+b) dx \quad (28)$$

$$- \int_0^\Lambda \varepsilon_0 \varepsilon_1 h(x) \mathbf{E}(\Gamma)(x, \Gamma(x)-b) \cdot \mathbf{E}_{\mathbf{J}_\rho}(x, \Gamma(x)-b) dx \quad (29)$$

$$- \int_0^\Lambda \int_{\Gamma(x)-b}^{\Gamma(x)+b} \varepsilon(\Gamma)(x, z) h(x) \frac{\partial \mathbf{E}(\Gamma)}{\partial z}(x, z) \cdot \mathbf{E}_{\mathbf{J}_\rho}(x, z) dx dz \quad (30)$$

$$- \int_0^\Lambda \int_{\Gamma(x)-b}^{\Gamma(x)+b} \varepsilon(\Gamma)(x, z) h(x) \mathbf{E}(\Gamma)(x, z) \cdot \frac{\partial \mathbf{E}_{\mathbf{J}_\rho}}{\partial z}(x, z) dx dz. \quad (31)$$

Before taking the limit $b \rightarrow 0$, we split the electric field on the curve $z = \Gamma(x)$ into a component that is in every point of the curve tangential to the curve, and a component that is in every point of the curve perpendicular to the curve: $\mathbf{E}(x, \Gamma(x)) = \mathbf{E}_\parallel(x, \Gamma(x)) + \mathbf{E}_\perp(x, \Gamma(x))$. Note that $\mathbf{E}_\parallel(x, \Gamma(x))$ is continuous across the curve, but that in the limit $b \rightarrow 0$, $\mathbf{E}_\perp(x, \Gamma(x))$ is discontinuous. Therefore, in the latter case, we have to distinguish between limiting values taken from above and below the curve, therefore we will write $\mathbf{E}(x, \Gamma(x) \pm 0) = \mathbf{E}_\parallel(x, \Gamma(x)) + \mathbf{E}_\perp(x, \Gamma(x) \pm 0)$.

We consider first the limit $b \rightarrow 0$ of the integrals in Eqs. (28) and (29) for the tangential component. Since this component is continuous across the interface we can take the limit $b \rightarrow 0$ to get

$$\begin{aligned} & \int_0^\Lambda \varepsilon_0 \varepsilon_2 h(x) \mathbf{E}_\parallel(\Gamma)(x, \Gamma(x)) \cdot \mathbf{E}_{\mathbf{J}_\rho, \parallel}(x, \Gamma(x)) dx \\ & - \int_0^\Lambda \varepsilon_0 \varepsilon_1 h(x) \mathbf{E}_\parallel(\Gamma)(x, \Gamma(x)) \cdot \mathbf{E}_{\mathbf{J}_\rho, \parallel}(x, \Gamma(x)) dx \\ & = \int_0^\Lambda \varepsilon_0 (\varepsilon_2 - \varepsilon_1) h(x) \mathbf{E}_\parallel(\Gamma)(x, \Gamma(x)) \cdot \mathbf{E}_{\mathbf{J}_\rho, \parallel}(x, \Gamma(x)) dx. \end{aligned} \quad (32)$$

The perpendicular component of the electric field is discontinuous across the interface, but the displacement field $\mathbf{D}_\perp = \varepsilon \mathbf{E}_\perp$ is continuous. We therefore have

$$\mathbf{E}_\perp(x, \Gamma(x)+0) - \mathbf{E}_\perp(x, \Gamma(x)-0) = \left(1 - \frac{\varepsilon_2}{\varepsilon_1}\right) \mathbf{E}_\perp(x, \Gamma(x)+0). \quad (33)$$

Using this, the sum of the integrals in Eqs. (28) and (29) become for the perpendicular component in the limit $b \rightarrow 0$:

$$\int_0^\Lambda \varepsilon_0 \varepsilon_2 \left(1 - \frac{\varepsilon_2}{\varepsilon_1}\right) h(x) \mathbf{E}_\perp(\Gamma)(x, \Gamma(x)+0) \cdot \mathbf{E}_{\mathbf{J}_\rho, \perp}(x, \Gamma(x)+0) dx. \quad (34)$$

One can alternatively also express the limit $b \rightarrow 0$ of integrals in Eqs. (28) and (29) in terms of the limiting value of the electric fields from below the curve. We omit the details.

Consider now the integrals in Eqs. (30) and (31) for the tangential field components. Since \mathbf{E}_{\parallel} and $\mathbf{E}_{\mathbf{J}_{\mathcal{O},\parallel}}$ are continuous as function of z , $\frac{\partial \mathbf{E}_{\parallel}(\Gamma)}{\partial z}(x, z)$ and $\frac{\partial \mathbf{E}_{\mathcal{O},\parallel}}{\partial z}(x, z)$ are possibly discontinuous across Γ but bounded. It can be shown that the bound is uniform in $b \rightarrow 0$, hence the integrals vanish in the limit $b \rightarrow 0$.

Next, we consider the case of the normal components. Since

$$\lim_{b \rightarrow 0} \frac{\partial \mathbf{E}_{\perp}(\Gamma)}{\partial z} = [\mathbf{E}_{\perp}(\Gamma+0) - \mathbf{E}_{\perp}(\Gamma-0)] \delta_{\Gamma}, \quad (35)$$

we can write Eq. (30) in the limit $b \rightarrow 0$, using Eq. (33), as:

$$- \int_0^{\Lambda} h(x) \varepsilon_0 \varepsilon_2 \left(1 - \frac{\varepsilon_2}{\varepsilon_1}\right) \mathbf{E}_{\perp}(\Gamma)(x, \Gamma(x)+0) \cdot \mathbf{E}_{\mathbf{J}_{\mathcal{O},\perp}}(x, \Gamma(x)+0) dx. \quad (36)$$

The integral in Eq. (31) for $b \rightarrow 0$ also equals Eq. (36). Summing up, the Gateaux derivative $\delta I(\Gamma; h)$ in Eq. (25) for a surface with a sharp material transition is given by

$$\begin{aligned} \delta I(\Gamma; h) = & -2\omega \varepsilon_0 \text{Im} \int_0^{\Lambda} h(x) [(\varepsilon_2 - \varepsilon_1) \mathbf{E}_{\parallel}(\Gamma)(x, \Gamma(x)) \cdot \mathbf{E}_{\mathbf{J}_{\mathcal{O},\parallel}}(x, \Gamma(x)) \\ & - \varepsilon_2 \left(1 - \frac{\varepsilon_2}{\varepsilon_1}\right) \mathbf{E}_{\perp}(\Gamma)(x, \Gamma(x)+0) \cdot \mathbf{E}_{\mathbf{J}_{\mathcal{O},\perp}}(x, \Gamma(x)+0)] dx. \end{aligned} \quad (37)$$

Hence for a given perturbation h of the curve Γ , the Gateaux derivative $\delta I(\Gamma; h)$ of the radiated intensity in a given direction $\hat{\mathbf{k}}$ is obtained by computing the fields $\mathbf{E}(\Gamma)$ of a unit amplitude incident plane wave with wave vector \mathbf{k} , either S- or P-polarized, and the field $\mathbf{E}_{\mathbf{J}_{\mathcal{O}}}$ radiated by the current density $\mathbf{J}_{\mathcal{O}}$ inside the active region \mathcal{O} . Hence, only two boundary value problems (per polarization) have to be solved on the unit cell to compute $\delta I(\Gamma; h)$.

For a surface function $\Gamma(x)$ defined by n parameters, the gradient of the intensity can be calculated using only one additional numerical simulation. Using standard finite differencing to compute the gradient from function values directly, n function evaluations are needed, i.e. $2n$ boundary value problems have to be solved.

Analogous to Eq. (26), the direction of steepest ascent $\tilde{h}(x)$ is now given by

$$\begin{aligned} \tilde{h}(x) = & -C \text{Im} [(\varepsilon_2 - \varepsilon_1) \mathbf{E}_{\parallel}(\Gamma)(x, \Gamma(x)) \cdot \mathbf{E}_{\mathbf{J}_{\mathcal{O},\parallel}}(x, \Gamma(x)) \\ & - \varepsilon_2 \left(1 - \frac{\varepsilon_2}{\varepsilon_1}\right) \mathbf{E}_{\perp}(\Gamma)(x, \Gamma(x)+0) \cdot \mathbf{E}_{\mathbf{J}_{\mathcal{O},\perp}}(x, \Gamma(x)+0)], \end{aligned} \quad (38)$$

where C is such that $\int_0^{\Lambda} \tilde{h}(x)^2 dx = 1$.

Acknowledgment

This work is supported by the Dutch Technology Foundation (STW) with project code STW-10301.